

SEYED ABDOLLAH EKRAMIRAD<sup>1</sup>, MOHAMMAD AZADI<sup>1\*</sup>,  
NASSER SHAMSKIA<sup>1</sup>

## THE EFFECTIVE PARAMETERS ON THE BEHAVIOUR OF TREATED SANDS BY MICROBIAL-INDUCED CALCITE PRECIPITATION UNDER UNDRAINED TRIAXIAL TEST

Nowadays, geotechnical specialists are focused on reinforcing soil engineering parameters using innovative and environmentally friendly methods. Microbial-Induced Calcite Precipitation is a ground improvement method for modifying soil strength, permeability, and stiffness; therefore, it can be vital to study the effective factors on the technique's efficiency and cost reduction. This study examined how biologically treated sands subjected to undrained triaxial loading responded to simultaneous changes in cementation solution molarity, optical density ( $OD_{600}$ ), and curing time. The triaxial experiments showed that the strength increased with the rise in the mentioned parameters. While the solution molarity and optical density had the highest and lowest effect on the soil improvement process, respectively, the optical density role was considerably low when the molarity was high. Increasing the molarity of the cementation solution resulted in a 45% increase in the peak stress ratio, while the optical density and curing time were constant. On the other hand, similar behaviour of dense sand and change in the response of cemented soil from strain-hardening to strain-softening were other notable observations of this study. In addition, the peak stress ratio at low strains increased with increasing the cementation level and then decreased to close to the amount of untreated sand with increasing strain.

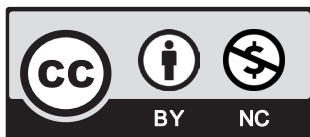
**Keywords:** MICP; Molarity; Optical density; Curing time; Triaxial test

## 1. Introduction

Soil biological treatment is a new improvement technique in geotechnical engineering that modifies soil physical and mechanical properties. In recent years, extensive research has been conducted on microbial-induced calcite precipitation (MICP) as a modern method to replace the

<sup>1</sup> DEPARTMENT OF CIVIL ENGINEERING, QAZVIN BRANCH, ISLAMIC AZAD UNIVERSITY, QAZVIN, IRAN

\* Corresponding author: [Azadi.mm98@gmail.com](mailto:Azadi.mm98@gmail.com)



© 2023. The Author(s). This is an open-access article distributed under the terms of the Creative Commons Attribution-NonCommercial License (CC BY-NC 4.0, <https://creativecommons.org/licenses/by-nc/4.0/deed.en>) which permits the use, redistribution of the material in any medium or format, transforming and building upon the material, provided that the article is properly cited, the use is noncommercial, and no modifications or adaptations are made.

injection of chemicals such as epoxy, acrylamide, phenoplasts, silicates, and polyurethane into the soil due to environmental concerns and high costs [1,2]. MICP can alter soil-engineering parameters based on the activity of urease-positive bacteria.

The bacteria used in this method are from the Bacillus family, which play the role of catalysts by producing calcium carbonate in the urea hydrolysis process (based on Eq. (1)) and are known as the Microbial Induced Calcite Precipitation (MICP) method [3]. Here, at first bacterial culture and growth in the laboratory are created by special face reactors, and then sedimentary bacteria are added directly to the soil [4].



Many studies have been carried out on the potential of this method in various fields, including biological remediation to improve sandy soil properties [5,6], seepage control in sandy soil [7], and remediation of concrete cracks [8,9]. Other works include optimising carbonate deposition in soil [10], erosion mitigation and stabilisation of sandy slopes [11,12], and production of “bio-bricks” treated at partial saturation conditions [13]. Controlled deposition of minerals into the soil voids has been significantly developed to change the macro-soil properties as a new innovative approach in geotechnical engineering [6]. Fig. 1 shows biological calcite deposition by hydrolysis of urea.

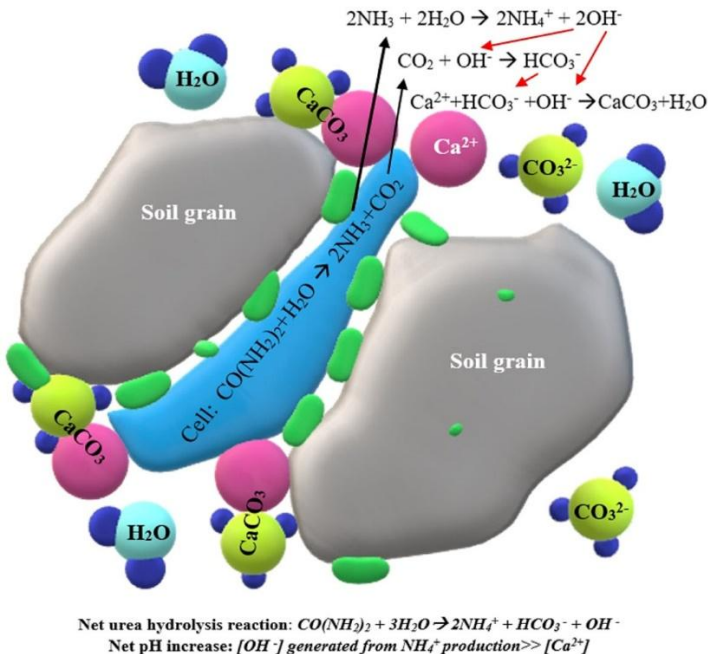


Fig. 1. Overview of biological calcite deposition by hydrolysis of urea

Research on the development of different biological improvement methods and the parameters affecting their efficiency continued. Harkes et al. [3] investigated the role of two-phase

injection to control a homogeneous distribution of bacterial activity and how to prevent clogging at the injection point. In another study, Al Qabany et al. [14] studied the effect of cementation concentration and retention time on the efficiency of the biological treatment method under constant optical density conditions. Montoya and Dejong [15] demonstrated the relationship between cementation level and the stress-strain behaviour of sands in the consolidated undrained (CU) triaxial test.

Other research in this field includes the desirable pH range from 7.5 to 8 [16]; the significant difference in urease activity between 20 to 28°C compared to lower temperatures [17]; the decrease of calcite deposition and soil strength by increasing the volume of injection to more than one-third of soil pores [18]; prevention of the clogging of bio-flocs formation by single-phase injection and low pH [19]; Long-term sustainability of MICP in aqueous media [20]; development of an improved immersing method through multiple treatments in low cementation media concentration [21]; the effects of cementation on the instability and critical state behaviours of Fraser river sand [22]; Effect of stress path on the shear response of bio-cemented sands [23]; Homogeneity and mechanical behaviours of sands improved by a temperature-controlled one-phase MICP method [24]; and Reduction of Brittleness of Fine Sandy Soil Biocemented by Microbial-Induced Calcite Precipitation [25].

By using biological improvement, it is possible to increase the resistance, and bearing capacity of the soil, as well as the surface tension of the soil against the wind. Rock acoustic experiments [26] can be used to assess MICP's effectiveness in repairing small rock cracks. Other applications of biological improvement include reducing the permeability of salt caves for the storage of natural gas, LPG, oil, hydrogen, and compressed air [27].

In this study, the favourable results of some parameters by previous researchers, such as pH, injection speed and retention time, were used, and in order to complete the previous works, the simultaneous effect of the parameters (including cementation solution molarity, the optical density of bacteria suspension, and curing time) on the stress-strain behaviour of the treated sand have been investigated. Also, the four-phase injection was used to control a homogeneous distribution of bacterial activity and prevent clogging at the injection point. For each of the parameters, three levels of variations were considered. After designing the experiment by Box-Behnken Design (BBD) [28], samples were prepared in a PVC mould. BBD is one of the most common designs used in response surface methodology (RSM) as a practical statistical optimisation design that has successfully been used in many biological and chemical processes [28]. Then, the undrained triaxial compression test (CU) was performed to evaluate the stress-strain behaviour of the improved sand and compare them, and the test outputs were presented as curves. Scanning electron microscope (SEM) images and X-Ray Diffraction (XRD) test results on the treated sample were also shown.

## 2. Materials

### 2.1. Soil type

In the first step, particle size analysis of the soil was carried out (Fig. 2). In Fig. 2, the percentage of particles passing through sieve No. 200 is about 4%, and the maximum diameter of the soil grain is 1.2 mm. The diameter of most soil grains is between 0.15-0.3 mm. According to the unified soil classification system, the soil was identified as SP soil, i.e. ASTM D2487

(Table 1). Geometric consistency between the bacterial size in the range of 0.5-3.0  $\mu\text{m}$  [29] and soil grains is an important factor in the MICP. According to Fig. 2 and the particle size range of the study, bacteria are capable of travelling through soil pores. Some characteristic soil parameters are presented in Table 1.

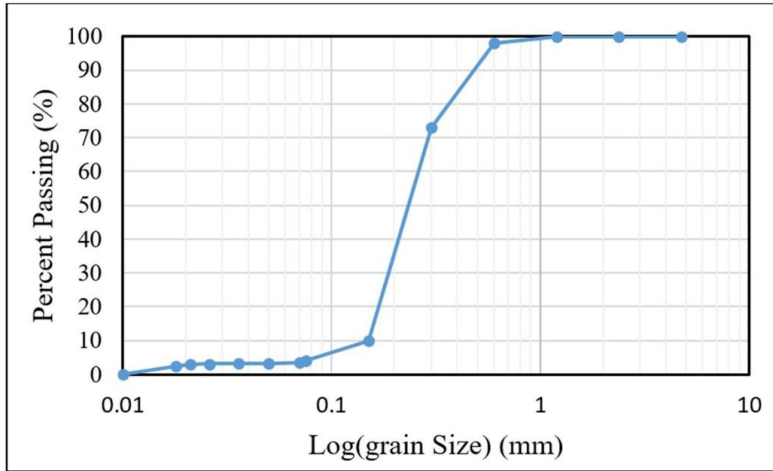


Fig. 2. The grain size distribution of material

TABLE 1

Physical properties of the material

Properties	GS	$\gamma_d$ ( $\text{g}/\text{cm}^3$ )	Dr	Cu	Cc
Value	2.63	1.54	0.37	1.62	0.74

GS: Solid particle density,  $\gamma_d$ : Dry unit weight of soil, Cu: Uniformity coefficient, Cc: Curvature coefficient.

## 2.2. Microorganism and culture medium

*Sporosarcina pasteurii* with positive urease activity was used as catalysts for the reaction. These lyophilized bacteria were obtained from Iran's scientific and industrial research centre and moved to the culture medium containing 15 g/L yeast extract and 5 g/L  $\text{NiCl}_2$  at a pH = 8.5 for activity. The culture medium was centrifuged (200 rpm) at 4000 g for 20 min in 20 ml volumes, washed in the fresh growth medium, and centrifuged again. The urease enzyme activity was measured by monitoring the rate of urea hydrolysis, according to Whifin's proposed method (2004), by measuring changes in electrical conductivity. The urease reaction involves the hydrolysis of non-ionic substrate urea to ionic products; thus, it increases the electrical conductivity under standard conditions [3]. Table 2 shows the characteristics of the culture medium used in this study.

Since one of the parameters in this work is the optical density of the bacterium suspension, it can be measured using a spectrophotometer at a wavelength of 600 nm [30]. Also, ammonium concentration was determined by a modified Nessler method [6].

### 2.3. Cementation solution

A cementation solution is needed to prepare the sample, which uses urea and calcium chloride compounds. For the formation of calcium carbonate precipitation in the intergranular space, a cementation solution was injected into the soil after preparation, where the compounds of urea (60 g/mol) and calcium chloride dihydrate (147 g/mol) were used based on the solution molarity (0.5, 1.0, and 1.5 mol/L). The required weight of urea and calcium chloride was calculated based on the pore volume of the cylindrical soil sample with a diameter and height of 7 and 14 cm, respectively, and an approximate solution volume of 250cc for each injection step. Then, after weighing and dissolving in distilled water, the cementation solution was prepared. To prepare the cementation solution, the weighted material is added to distilled water and dissolved. After preparing the solution, it is kept in the laboratory and used in different injection stages. For injection, the cementation solution was poured into a container. The container is placed on top of the sample, and the solution is injected into the sample under the force of gravity through a valve installed at the bottom of the container.

## 3. Method

### 3.1. Sample preparation

The specimens were prepared in a cylindrical mould with a diameter and height of 7 and 14 cm according to the conditions of the triaxial apparatus. The air pluviation method has been used to make the sample in the laboratory. To drain the cementation solution at the end of each injection phase, it is necessary to embed an outlet port on the bottom of the mould that can be opened and closed (with a suitable filter to prevent soil passage). After making and sealing the mould, the soil sample was replaced according to standard conditions with a relative density of 0.37 and an equivalent weight of 820 g.

### 3.2. Biological treatment process

For uniform distribution of calcite precipitation, sample improvement was performed by the gravity injection method after the sample was inserted into the mould. Here, a 4-phase injection was used to prevent clogging and control the uniform distribution of  $\text{CaCO}_3$  precipitation. The biological treatment steps were followed below:

- Washing the sample with distilled water equals the soil volume based on some research [6,31].
- The gravity injection of diluted bacteria (in 250 mL) with buffers and culture medium is equivalent to 1.2 times the pore volume [32,33].
- Bacterial immobilisation by calcium chloride solution equal to 1.2 times the pore volume based on the molarity of each experiment [3].
- After 6 hours, the first and second steps of cementation solution injection were performed according to the urea- $\text{CaCl}_2$  input rate equal to 0.042 mol/L/h (Based on reference) [14]. Drainage of the cementation solution from the mould end valve is taken at the end of each injection stage.
- Re-infusion of bacteria with buffers and culture medium.

- Injection of the third phase of the cementation solution, followed by the draining of it.
- Injection of the fourth phase of the cementation solution.
- The final drainage of the cementation solution from the mould end valve is taken after approximately 48 hours.

After completing the injection process, the specimen was kept in the laboratory at 27 to 30°C according to the curing time (15, 30, and 45 days) to complete the biological remediation process.

### 3.3. Triaxial test process

The prepared specimens to perform a triaxial test according to ASTM D4767-CU are placed in a triaxial device (Fig. 3). The soil sample is completely saturated by reaching Skempton's coefficient B to 0.95. Then the sample was consolidated at the confinement stress of 100 kPa. After closing the outlet valves at the bottom of the sample, the loading under deviation stresses continued until the strain was equal to 20%. During loading, the computer stored the device's outputs for short periods, and then statistical analysis was performed on them. Finally, SEM images were taken to investigate the deposition of calcite crystals on the samples, and then XRD analysis was carried out on them.

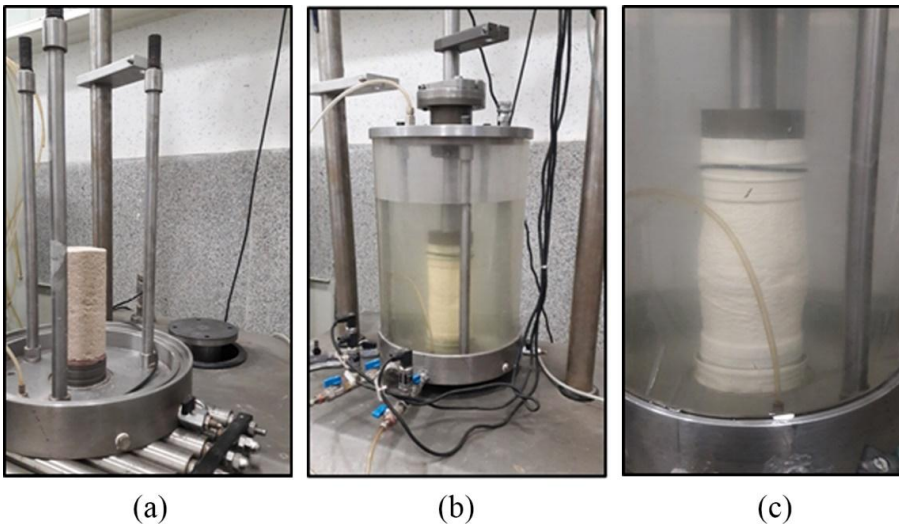


Fig. 3. Triaxial test according to ASTM D4767-CU: (a) Treated sand (b) Sample during loading (c) End of experiment

## 4. Result and discussion

In this study, experiment design was performed using Design Expert ver. 11.0.3.0 software to optimise the number of experiments (to reduce costs). The main variables included cementation solution molarity, optical density, and curing time (three levels of variation according to Table 2);

the number of trials was reduced from 27 to 17 based on the BOX-Behnken Design (BBD) with five central points. In this study, due to the statistical work on biological improvement, the BBD method is more appropriate. According to these experiments, the following results were obtained.

TABLE 2

Level of independent variables for MICP by the Box-Behnken Design (BBD)

Parameters	Cementation solution molarity (mol/L)	Optical density ( $OD_{600}$ )	Curing time (day)
Level of variations	0.5	0.8 – 1.2	15
	1.0	1.5 – 2.0	30
	1.5	2.0 – 4.0	45

#### 4.1. The behaviour of improved sands in undrained triaxial compression

Undrained triaxial tests were performed to study the effect of the below parameters on MICP treated soil subjected to undrained loading. The response of the untreated sand was plotted as a reference to compare sample #4 (a soil with maximum cementation) in Fig. 4. The values of deviation stress and mean effective stress are defined herein, namely  $q = \sigma_1 - \sigma_3$  and  $p' = (\sigma_1' + 2\sigma_3')/3$ .

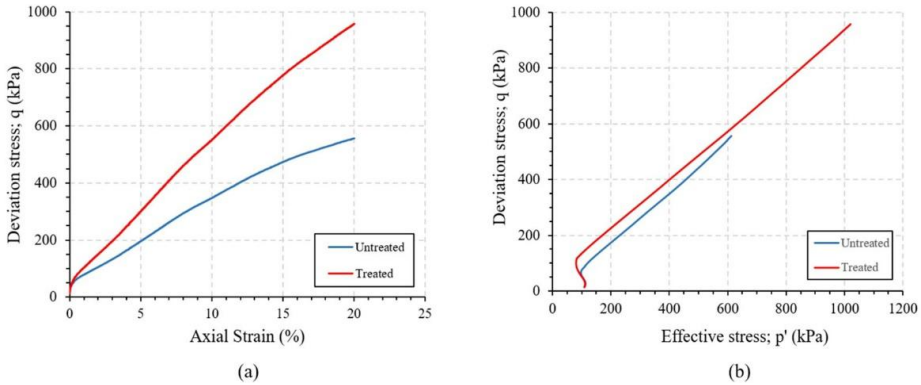


Fig. 4. The effect of solution molarity on biological cemented sand (in treated sand: 1.5 M,  $OD_{600} = 2.0-4.0$ , and curing time = 30 days): (a) Deviation stress (b) Effective stress path

The maximum values of  $q$  and  $p'$  are 957 kPa and 1020 kPa for improved sand, respectively. Compared to untreated soil, an increase of 72 and 67 percent was observed in  $q$  and  $p'$  values, respectively. For comparison, treated and untreated sand samples were subjected to undrained loading. Then the curves of deviation stress ( $q$ )/effective stress ( $p'$ ) and pore water pressure (PWP) versus axial strain have been shown in Figs. 5 to 7.

The maximum peak stress ratio ( $q/p'$ ) happened at low strains; finally, the stress ratio decreases until it comes close to clean sand. The most variations in  $q/p'$  were observed in sample #4, which was approximately 50% clean soil. The changes in peak stress ratio in cemented sands



were similar to dense sand specimens; however, the strain-softening happened after the peak stress. The negative pore water pressure was developed to a strain of approximately 1.5%. Also, the dilative tendencies in improved soils were seen, which could be due to the brittle cementation at the particle contact location.

#### 4.1.1. Solution Molarity

One of the effective parameters on the stress-strain behaviour of cemented sands is the solution molarity. As shown in Fig. 4, as the molarity of the cementation solution increases, the amount of peak stress ratio ( $q/p'$ ) increases, but the PWP first increases and then decreases. The rate of change in PWP is low at the low molarity level.

Changes in the peak stress ratio ( $q/p'$ ) and pore water pressure in Fig. 5 show that increasing the molarity of the cementation solution has a significant effect on microbial-induced calcite precipitation. In Fig. 5(a), a comparison of curves 1 and 2 (also 3 and 4) shows that  $q/p'$  changes are approximately 45%. On the other hand, strain hardening is not observed in sample #1. But, the above phenomenon occurs in sample #4 due to the stronger contact band with increasing molarity to 1.5, which occurs almost at the low strain level. Biologically improved specimens have a softening strain with increasing strain, and their peak stress ratio decreases. However, biologically improved specimens are always ruptured at the level of peak stress ratio above the unimproved state, which is quite evident in Fig. 5(a). As shown in Fig. 5(b), the improved samples are first exposed to increased pore water pressure, and then their values are reduced (similar to the behaviour of compacted sand). Its value for sample #4 has reached about  $-300$  kPa.

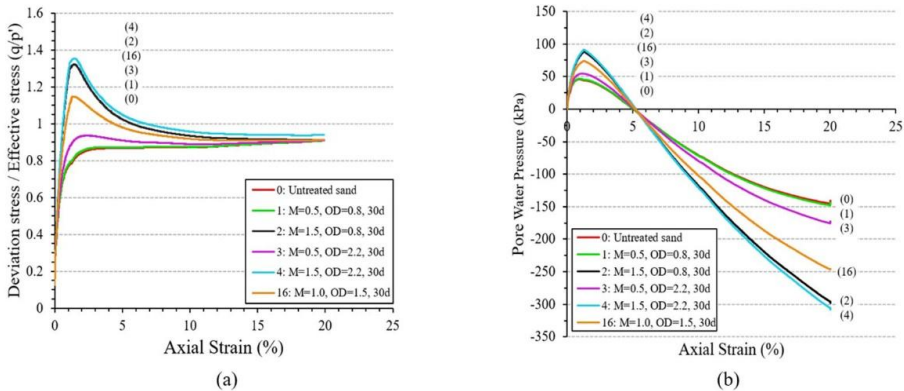


Fig. 5. The effect of solution molarity on biological cemented sand:  
(a) Peak stress ratio (b) Pore Water Pressure

#### 4.1.2. Optical Density

The effect of another parameter on treated sand behaviour is observed in Fig. 6. Simultaneous comparison of Figs. 6(a) and 6(c) states that: firstly, the effect of optical density on increasing the peak stress ratio was about 4% when the molarity of the cementation solution is low (comparison of curves 1 and 3). Secondly, in the initial curing time (up to 15 days) and when the molarity is high, the dominant parameter in increasing the degree of cementation and resistance is the



molarity. As can be seen, the optical density has a negligible effect, but with increasing sample age, its impact becomes greater (though slight).

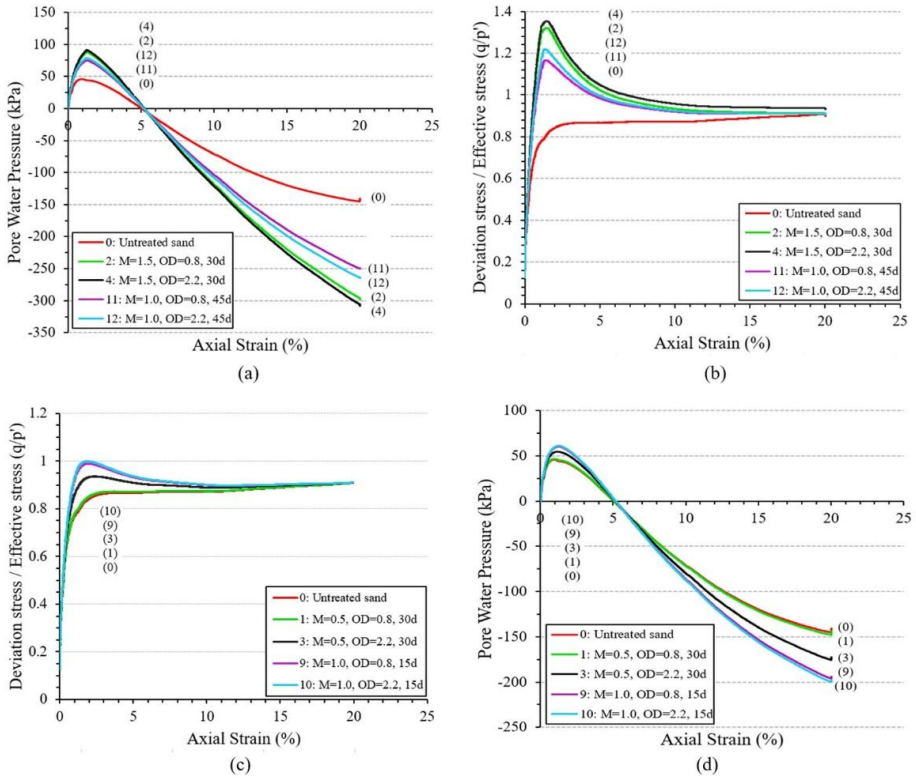


Fig. 6. The effect of optical density on biological cemented sand: (a) Peak stress ratio (b) Pore Water Pressure (c) Peak stress ratio (d) Pore Water Pressure

Calculations show that the changes of  $q/p'$  versus optical density after improvement for samples with 0.5, 1.0, and 1.5 molarity at the curing time of 30 days are 3%, 26%, and 49%, respectively. But, with decreasing the curing time, it tends to zero. The process of PWP changes versus axial strain in Figs. 6(b) and 6(d) are similar to the previous section and related to the sand cementation level. At first, the negative pore pressure increases (Similar to the behaviour of compacted sand), and then with the faster drop in heavily cemented samples, its value in sample #4 reaches 350 kPa. A comparison of samples 1 and 3 in Fig. 6(d) shows that with changes in optical density (same conditions for low cementation solution molarity and curing time), the PWP increases by about 22%.

#### 4.1.3. Curing Time

To investigate the effect of sample curing time on biological cementation, curing time was evaluated for 15, 30, and 45 days. Evidence shows that by increasing the curing time from

15 to 45 days under similar conditions for cementation solution molarity and optical density, the peak stress ratio can be increased by up to 22% (curves 10 and 12 in Fig. 7). In addition, due to the relatively low effect of bacterial optical density in high molarity samples, the comparison of the results shows that the most significant effect of curing time occurred after 30 days. Then the rate of normalised deviation stress changes decreases.

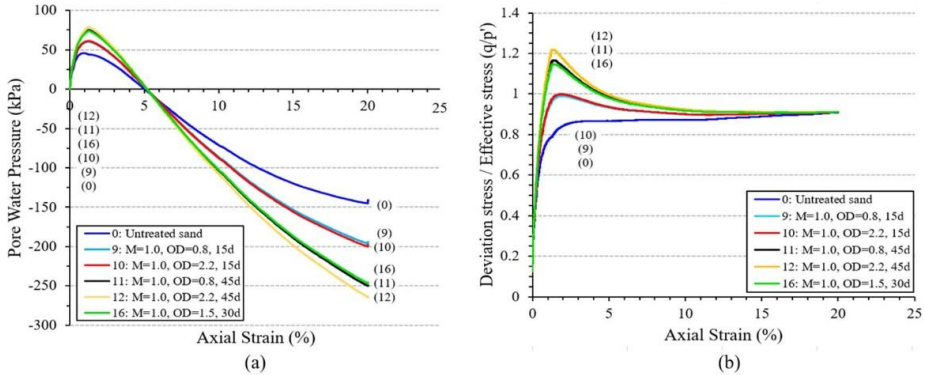


Fig. 7. The effect of curing time on biological cemented sand: (a) Peak stress ratio (b) Pore Water Pressure

On the other hand, for the biologically improved sample, the curing time has little effect on the cementation process of the samples if the solubility molarity and optical density are low. Also, under the same conditions of solution molarity and optical density of bacteria, the peak stress ratio of the samples will reach the maximum value after the curing time between 30 to 35 days.

Next, the results of pore water pressure changes were examined in Fig. 7(b). As expected, the trend of changes in pore water pressure under the influence of curing time was similar to the previous sections (pore water pressure first increased and then decreased). Again, most of the changes in pore water pressure occurred between 30 and 35 days, and then, the rate of increase in pore water pressure decreased. Also, a comparison of samples 10 and 12 in Fig. 7(b) shows that increasing the curing time from 15 to 45 days has led to a 34% increase in pore water pressure. Similar to normalised deflection stress changes, at low molarity levels, increasing the curing time did not have a significant effect on the trend of pore water pressure changes.

## 4.2. Assessment of SEM results

The SEM images in Fig. 8 show calcite precipitation on soil surfaces. Fig. 8 shows that the idealised  $\text{CaCO}_3$  distributions can occur in the grain contact location. Here, contact bands are seen at the connection of grains in the treated soil under saturated conditions.

Fig. 9 shows the SEM pictures of the improved sands with various levels of molarity and optical density. A comparison of Figs. 9(a), 9(b), and 9(c) show that increasing molarity of the cementation solution results in more  $\text{CaCO}_3$  deposition on the surface and inside the soil voids, and stronger contact bonds are formed, leading to an increase in the strength and stiffness of biologically treated samples. On the other hand, Fig. 9(a) shows that reducing the molarity of the cementation solution causes the formation of partial calcite precipitation between the grains, which

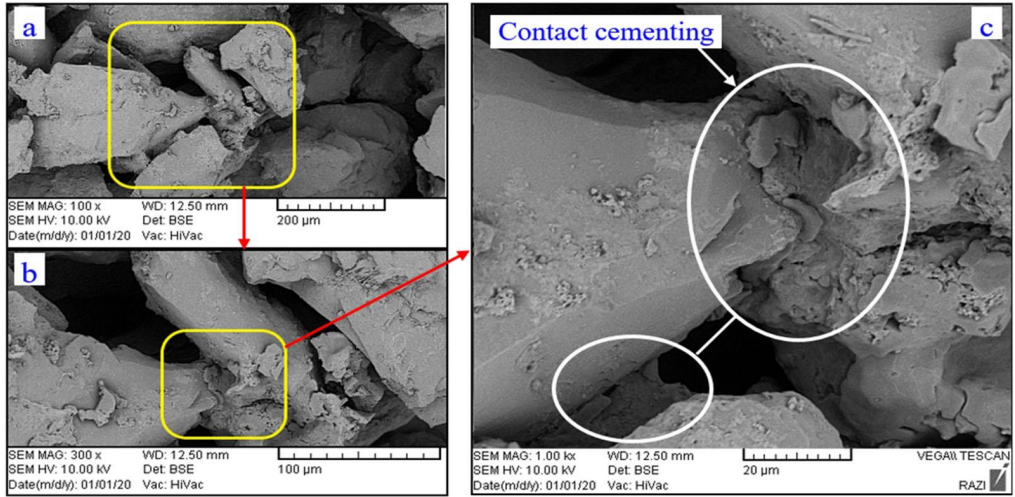


Fig. 8. Scanning Electron Microscope (SEM) images for cemented sand ( $M = 1.5$  mol,  $OD_{600} = 1.5-2.0$ ) at magnifications of (a) 100 $\times$ ; (b) 300 $\times$ ; (c) 1000 $\times$

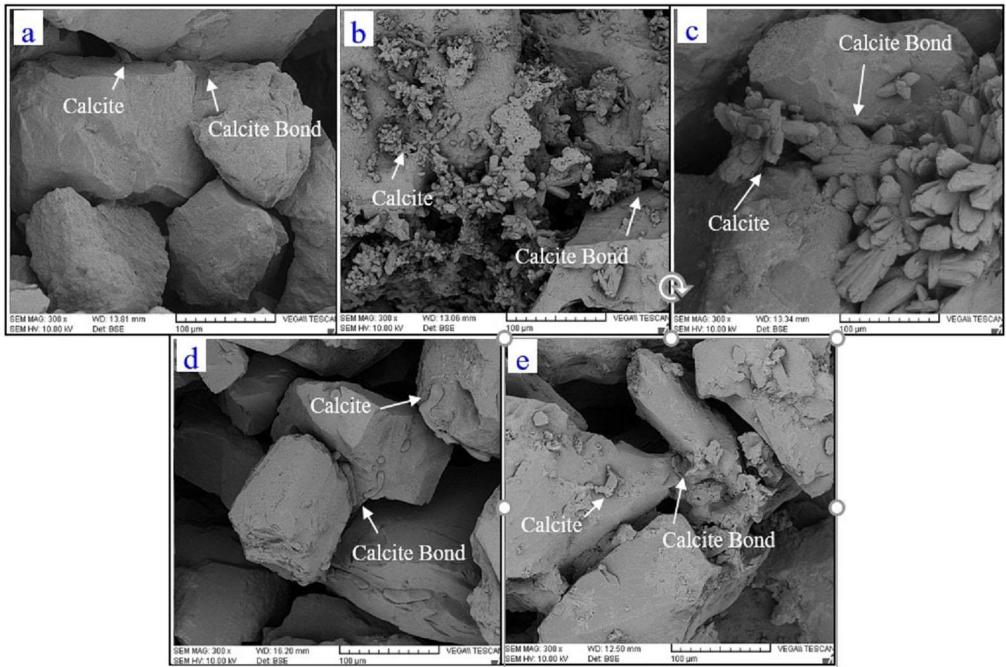


Fig. 9. Scanning Electron Microscope (SEM) images to compare cemented sands at magnifications of 300 $\times$ :  
 (a) 0.5 M,  $OD_{600} = 2.0-4.0$  (b) 1.0 M,  $OD_{600} = 2.0-4.0$  (c) 1.5 M,  $OD_{600} = 2.0-4.0$   
 (d) 1.5 M,  $OD_{600} = 0.8-1.2$  (e) 1.5 M,  $OD_{600} = 1.5-2.0$

will not have a great effect on increasing the strength of the treated sample. But in Fig. 9(c), the amount of sediment formation at the junction and on the surface of the grains is clearly visible. Furthermore, the comparison of Figs. 9(c), 9(d), and 9(e) confirm the increase in calcite formation with increasing optical density. However, these changes are not as significant as the molarity.

### 4.3. X-Ray Diffraction (XRD) analysis

XRD analysis investigated the physical changes inside the soil particles due to the cementation. XRD is a technique employed to identify the crystal structure of a material, where different crystalline atoms result in different diffraction patterns for an incident X-ray beam [34]. Fig. 10 shows the Brogg angle of refraction ( $\theta$ ) and the relative intensity of X-ray diffraction inside the crystal for five sand samples. The characteristic diffraction peaks are observed at  $2\theta$  diffraction angles of  $23.15^\circ$ ,  $29.39^\circ$ ,  $32.74^\circ$ ,  $35.99^\circ$ ,  $39.24^\circ$ ,  $43.30^\circ$ ,  $47.51^\circ$ , etc. A gradual increase in the intensity of the peaks on  $2\theta = 29.39^\circ$  shows clearly the increase in  $\text{CaCO}_3$  precipitation production with the increase in molarity from 0.5 to 1.5, which can cause stronger contact bands and increase the resistance parameters of biologically cemented soil. The rate of change of diffraction peaks with increasing molarity is particularly high because Fig. 10 clearly shows that molarity has a more substantial impact on the process of biological improvement than does the optical density of bacteria. But, these changes are not significant with the increasing optical density of bacteria.

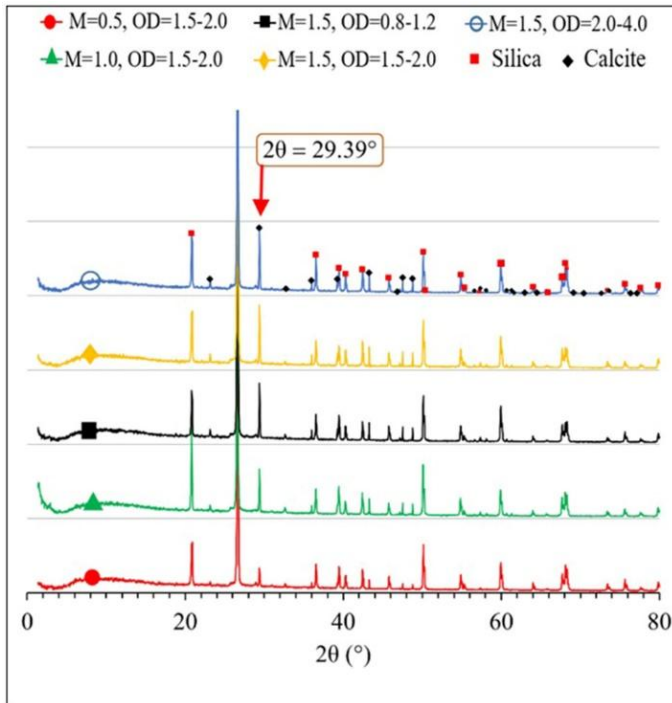


Fig. 10. X-Ray Diffraction (XRD) analysis for cemented sand (M: solution molarity, OD: Optical Density)

## 5. Conclusions

This paper has studied the effect of solution molarity, optical density ( $OD_{600}$ ), and curing time on the stress-strain behaviour of biological cemented sands. The specimens were subjected to undrained loading with confinement of 100 kPa. The results of this research are as follows:

- The effect of solution molarity and optical density on treated sand resistance was 68.7% and 7.5%, respectively. This indicates that the impact of molarity is much greater than the optical density.
- The improved soils showed a significant increase in strength, also dilative tendencies to pre-treatment. In addition, the peak stress ratio ( $q/p'$ ) happened in a strain of about 1%, while its values increased with the cementation level.
- It was found that the maximum deviation stress ( $q$ ) at small strains reduces as the cementation decreases, and the transition from strain-hardening to strain-softening behaviour occurs with the strain increases. The breaking of the contact bands between the particles has caused this behaviour change.
- The negative pore pressure in the greater cemented sands increased faster due to more  $CaCO_3$  precipitation and stronger bond formation. Then it decreased more quickly because of the breaking of the particle contact bonds and the increase of correlation between soil pores.
- The effect of optical density is more pronounced in low molarity samples. In addition, its impact increased the rise of curing time due to more opportunities for the cementation process.
- Most of the effect of the curing time was after 30 days. If the molarity and optical density are low, the curing time will not have much effect on soil improvement.
- The SEM images and XRD tests showed that increased molarity and optical density lead to more  $CaCO_3$  deposition on the surface and inside the soil voids, and stronger contact bonds are formed. However, the impact of molarity is still more significant.
- The results of the impact of the above parameters on MICP can be used to optimise the biological improvement process. The use of biological improvement is used to increase the strength and stiffness and reduce the permeability of the soil.

## Acknowledgments

This work is part of a research project funded by Qazvin Azad University.

## References

- [1] R.H. Karol, Chemical grouting and soil stabilization, revised and expanded. Crc Press (2003).
- [2] P.P. Xanthakos, L.W. Abramson, D.A. Bruce, Ground control and improvement, John Wiley & Sons (1994).
- [3] M.P. Harkes, L.A. Van Paassen, J.L. Booster, V.S. Whiffin, M.C. van Loosdrecht, Fixation and distribution of bacterial activity in sand to induce carbonate precipitation for ground reinforcement. *Ecological Engineering* **36** (2), 112-117 (2010). DOI: <https://doi.org/10.1016/j.ecoleng.2009.01.004>
- [4] J.T. DeJong, B.M. Mortensen, B.C. Martinez, D.C. Nelson, Bio-mediated soil improvement. *Ecological Engineering* **36** (2), 197-210 (2010). DOI: <https://doi.org/10.1016/j.ecoleng.2008.12.029>



- [5] J.T. DeJong, M.B. Fritzges, K. Nüsslein, Microbially induced cementation to control sand response to undrained shear. *Journal of Geotechnical and Geoenvironmental Engineering* **132** (11), 1381-1392 (2006). DOI: [https://doi.org/10.1061/\(ASCE\)1090-0241\(2006\)132:11\(1381\)](https://doi.org/10.1061/(ASCE)1090-0241(2006)132:11(1381))
- [6] V.S. Whiffin, L.A. Van Paassen, M.P. Harkes, Microbial carbonate precipitation as a soil improvement technique. *Geomicrobiology Journal* **24** (5), 417-423 (2007). DOI: <https://doi.org/10.1080/01490450701436505>
- [7] Y. Gao, X. Tang, J. Chu, J. He, Microbially induced calcite precipitation for seepage control in sandy soil. *Geomicrobiology Journal* **36** (4), 366-375 (2019). DOI: <https://doi.org/10.1080/01490451.2018.1556750>
- [8] M. Luo, C.X. Qian, R.Y. Li, Factors affecting crack repairing capacity of bacteria-based self-healing concrete. *Construction and Building Materials* **87**, 1-7 (2015). DOI: <https://doi.org/10.1016/j.conbuildmat.2015.03.117>
- [9] V. Achal, A. Mukherjee, M.S. Reddy, Microbial concrete: way to enhance the durability of building structures. *Journal of Materials n Civil Engineering* **23** (6), 730-734 (2011). DOI: [https://doi.org/10.1061/\(ASCE\)MT.1943-5533.0000159](https://doi.org/10.1061/(ASCE)MT.1943-5533.0000159)
- [10] G.D.O. Okwadha, J. Li, Optimum conditions for microbial carbonate precipitation. *Chemosphere* **81** (9), 1143-1148 (2010). DOI: <https://doi.org/10.1016/j.chemosphere.2010.09.066>
- [11] N.J. Jiang, K. Soga, The applicability of microbially induced calcite precipitation (MICP) for internal erosion control in gravel-sand mixtures. *Géotechnique* **67** (1), 42-55 (2017). DOI: <https://doi.org/10.1680/jgeot.15.P.182>
- [12] E. Salifu, E. MacLachlan, K.R. Iyer, C.W. Knapp, A. Tarantino, Application of microbially induced calcite precipitation in erosion mitigation and stabilisation of sandy soil foreshore slopes: A preliminary investigation. *Engineering Geology* **201**, 96-105 (2016). DOI: <https://doi.org/10.1016/j.enggeo.2015.12.027>
- [13] L. Cheng, T. Kobayashi, M.A. Shahin, Microbially induced calcite precipitation for production of "bio-bricks" treated at partial saturation condition. *Construction and Building Materials* **231**, 117095 (2020). DOI: <https://doi.org/10.1016/j.conbuildmat.2019.117095>
- [14] A. Al Qabany, K. Soga, C. Santamarina, Factors affecting efficiency of microbially induced calcite precipitation. *Journal of Geotechnical and Geoenvironmental Engineering* **138** (8), 992-1001 (2012). DOI: [https://doi.org/10.1061/\(ASCE\)GT.1943-5606.0000666](https://doi.org/10.1061/(ASCE)GT.1943-5606.0000666)
- [15] B.M. Montoya, J.T. DeJong, Stress-strain behavior of sands cemented by microbially induced calcite precipitation. *Journal of Geotechnical and Geoenvironmental Engineering* **141** (6), 04015019 (2015). DOI: [https://doi.org/10.1061/\(ASCE\)GT.1943-5606.0001302](https://doi.org/10.1061/(ASCE)GT.1943-5606.0001302)
- [16] G. Kim, J. Kim, H. Youn, Effect of temperature, pH, and reaction duration on microbially induced calcite precipitation. *Applied Sciences* **8** (8), 1277 (2018). DOI: <https://doi.org/10.3390/app8081277>
- [17] W. De Muynck, K. Verbeken, N. De Belie, W. Verstraete, Influence of temperature on the effectiveness of a biogenic carbonate surface treatment for limestone conservation. *Applied Microbiology and Biotechnology* **97** (3), 1335-1347 (2013). DOI: <https://doi.org/10.1007/s00253-012-3997-0>
- [18] K. Rowshanbakht, M. Khamsehchian, R.H. Sajedi, M.R. Nikudel, Effect of injected bacterial suspension volume and relative density on carbonate precipitation resulting from microbial treatment. *Ecological Engineering* **89**, 49-55 (2016). DOI: <https://doi.org/10.1016/j.ecoleng.2016.01.010>
- [19] L. Cheng, M.A. Shahin, J. Chu, Soil bio-cementation using a new one-phase low-pH injection method. *Acta Geotechnica* **14** (3), 615-626 (2019). DOI: <https://doi.org/10.1007/s11440-018-0738-2>
- [20] D. Gat, Z. Ronen, M. Tsesarsky, Long-term sustainability of microbial-induced CaCO<sub>3</sub> precipitation in aqueous media. *Chemosphere* **184**, 524-531 (2017). DOI: <https://doi.org/10.1016/j.chemosphere.2017.06.015>
- [21] K. Wen, Y. Li, S. Liu, C. Bu, L. Li, Development of an improved immersing method to enhance microbial induced calcite precipitation treated sandy soil through multiple treatments in low cementation media concentration. *Geotechnical and Geological Engineering* **37** (2), 1015-1027 (2019). DOI: <https://doi.org/10.1007/s10706-018-0669-6>
- [22] G.A. Riveros, A. Sadrekarimi, Effect of microbially induced cementation on the instability and critical state behaviours of Fraser River sand. *Canadian Geotechnical Journal* **57** (12), 1870-1880 (2020). DOI: <https://doi.org/10.1139/cgj-2019-0514>
- [23] A. Nafisi, Q. Liu, B.M. Montoya, Effect of stress path on the shear response of bio-cemented sands. *Acta Geotechnica* **16** (10), 3239-3251 (2021). DOI: <https://doi.org/10.1007/s11440-021-01286-7>
- [24] Y. Xiao, Y. Wang, S. Wang, T.M. Evans, A.W. Stuedlein, J. Chu, H. Liu, Homogeneity and mechanical behaviors of sands improved by a temperature-controlled one-phase MICP method. *Acta Geotechnica* **16** (5), 1417-1427 (2021). DOI: <https://doi.org/10.1007/s11440-020-01122-4>

- [25] X. Wang, C. Li, W. Fan, H. Li, Reduction of Brittleness of Fine Sandy Soil Biocemented by Microbial-Induced Calcite Precipitation. *Geomicrobiology Journal* 1-13 (2022). DOI: <https://doi.org/10.1080/01490451.2021.2019858>
- [26] Dong, Longjun, Yongchao Chen, Daoyuan Sun, and Yihan Zhang, Implications for rock instability precursors and principal stress direction from rock acoustic experiments. *International Journal of Mining Science and Technology* **31** (5), 789-798 (2021). DOI: <https://doi.org/10.1016/j.ijmst.2021.06.006>
- [27] K. Cyran, The influence of impurities and fabrics on mechanical properties of rock salt for underground storage in salt caverns – a review. *Archives of Mining Sciences* **66** (2), (2021). DOI: <https://doi.org/10.24425/ams.2021.137454>
- [28] A.I. Khuri, S. Mukhopadhyay, Response surface methodology. *Wiley Interdisciplinary Reviews: Computational Statistics* **2** (2), 128-149 (2010). DOI: <https://doi.org/10.1002/wics.73>
- [29] J. Madigan, M.T. Martinko, Brock biology of microorganisms, 11th ed (2003).
- [30] L. Chen, L. Li, F. Xing, J. Peng, K. Peng, Y. Wang, Z. Xiang, Human urine-derived stem cells: potential for cell-based therapy of cartilage defects. *Stem Cells International*. (2018). DOI: <https://doi.org/10.1155/2018/4686259>
- [31] H. Lin, M.T. Suleiman, D.G. Brown, E. Kavazanjian, Mechanical behavior of sands treated by microbially induced carbonate precipitation. *Journal of Geotechnical and Geoenvironmental Engineering* **142** (2), 04015066 (2016). DOI: [https://doi.org/10.1061/\(ASCE\)GT.1943-5606.0001383](https://doi.org/10.1061/(ASCE)GT.1943-5606.0001383)
- [32] T. Sasaki, R. Kuwano, Undrained cyclic triaxial testing on sand with non-plastic fines content cemented with microbially induced CaCO<sub>3</sub>. *Soils and Foundations* **56** (3), 485-495 (2016). DOI: <https://doi.org/10.1016/j.sandf.2016.04.014>
- [33] Z. Han, X. Cheng, Q. Ma, An experimental study on dynamic response for MICP strengthening liquefiable sands. *Earthquake Engineering and Engineering Vibration* **15** (4), 673-679 (2016). DOI: <https://doi.org/10.1007/s11803-016-0357-6>
- [34] M. Azadi, M. Ghayoomi, N. Shamskia, H. Kalantari, Physical and mechanical properties of reconstructed biocemented sand. *Soils and Foundations* **57** (5), 698-706 (2017). DOI: <https://doi.org/10.1016/j.sandf.2017.08.002>